Resource

Cell Reports

Native CRISPR-Cas-Mediated Genome Editing Enables Dissecting and Sensitizing Clinical Multidrug-Resistant *P. aeruginosa*

Graphical Abstract

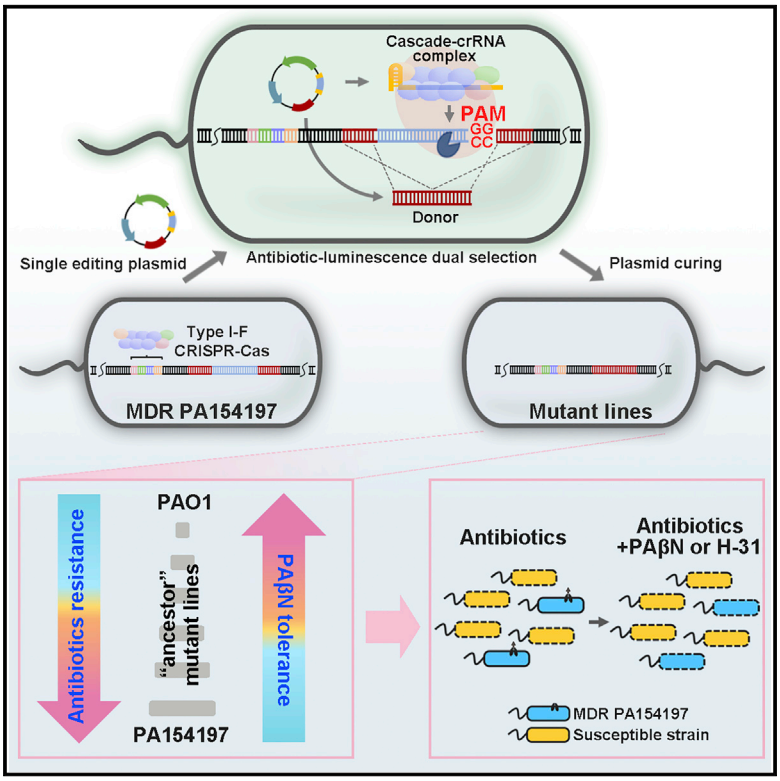

Highlights

- Endogenous type I-F CRISPR-Cas is repurposed for genome editing in MDR *P. aeruginosa*
- Mutant lines reveal key MDR determinants and extensive synergy in a clinical isolate
- Clinical strain PA154197 displays collateral sensitivity to small cationic peptidomimetics
- Small cationic peptidomimetics sensitize PA154197 cells to antibiotics

Authors

Zeling Xu, Ming Li, Yanran Li, ..., Patrick C.Y. Woo, Hua Xiang, Aixin Yan

Correspondence

xiangh@im.ac.cn (H.X.), ayan8@hku.hk (A.Y.)

In Brief

Xu et al. develop an efficient genome-editing technique in genetically recalcitrant clinical and environmental *P. aeruginosa* strains by exploiting their endogenous type I-F CRISPR-Cas system. Employing the technique, they identify underlying resistance mechanisms of an epidemic MDR genotype, PA154197, efficiently and develop anti-resistance strategies based on collateral sensitivity.

Xu et al., 2019, Cell Reports *29*, 1707–1717
November 5, 2019
https://doi.org/10.1016/j.celrep.2019.10.006

CellPress

Cell Reports
Resource

Native CRISPR-Cas-Mediated Genome Editing Enables Dissecting and Sensitizing Clinical Multidrug-Resistant *P. aeruginosa*

Zeling Xu,[1,6] Ming Li,[2,6] Yanran Li,[1] Huiluo Cao,[1,7] Lu Miao,[3] Zhaochao Xu,[3] Yusuke Higuchi,[4] Seiji Yamasaki,[4] Kunihiko Nishino,[4] Patrick C.Y. Woo,[5] Hua Xiang,[2,*] and Aixin Yan[1,8,*]

[1]School of Biological Sciences, The University of Hong Kong, Pokfulam Road, Hong Kong SAR, China
[2]State Key Laboratory of Microbial Resources, Institute of Microbiology, Chinese Academy of Sciences, Beijing 100101, China
[3]CAS Key Laboratory of Separation Science for Analytical Chemistry, Dalian Institute of Chemical Physics, Chinese Academy of Sciences, Dalian 116023, China
[4]Institute of Scientific and Industrial Research, Osaka University, Osaka 567-0047, Japan
[5]Department of Microbiology, Li Ka Shing Faculty of Medicine, The University of Hong Kong, Hong Kong SAR, China
[6]These authors contributed equally
[7]Present address: Department of Microbiology, Li Ka Shing Faculty of Medicine, The University of Hong Kong, Hong Kong SAR, China
[8]Lead Contact
*Correspondence: xiangh@im.ac.cn (H.X.), ayan8@hku.hk (A.Y.)
https://doi.org/10.1016/j.celrep.2019.10.006

SUMMARY

Despite being fundamentally important and having direct therapeutic implications, the functional genomics of the clinical isolates of multidrug-resistant (MDR) pathogens is often impeded by the lack of genome-editing tools. Here, we report the establishment of a highly efficient, *in situ* genome-editing technique applicable in clinical and environmental isolates of the prototypic MDR pathogen *P. aeruginosa* by harnessing the endogenous type I-F CRISPR-Cas systems. Using this approach, we generate various reverse mutations in an epidemic MDR genotype, PA154197, and identify underlying resistance mechanisms that involve the extensive synergy among three different resistance determinants. Screening a series of "ancestor" mutant lines uncovers the remarkable sensitivity of the MDR line PA154197 to a class of small, cationic peptidomimetics, which sensitize PA154197 cells to antibiotics by perturbing outer-membrane permeability. These studies provide a framework for molecular genetics and anti-resistance drug discovery for clinically isolated MDR pathogens.

INTRODUCTION

Antimicrobial resistance (AMR) is imposing an alarming threat on global public health. Particularly challenging are those "ESKAPE" pathogens that constitute the major sources of nosocomial infections with extraordinary drug resistance (i.e., *Enterococcus spp.*, *Staphylococcus aureus*, *Klebsiella spp.*, *Acinetobacter baumannii*, *Pseudomonas aeruginosa*, and *Enterobacter spp.*). Among them, *Pseudomonas aeruginosa* is recognized as a prototypical multidrug-resistant (MDR) pathogen owing to both its intrinsic resistance to a variety of antimicrobials and its enormous capacity to develope acquired resistance during antibiotics chemotherapies (Oliver et al., 2015; Poole, 2011; Santajit and Indrawattana, 2016; Stover et al., 2000). Remarkably, in recent years, MDR international high-risk clones of *P. aeruginosa* have emerged and caused worldwide outbreaks (Oliver et al., 2015). Hence, it is of paramount importance to deeply understand the resistance mechanisms of these clones and develop anti-resistance treatment strategies. However, these studies are frequently impeded because of the lack of genetic-editing tools in the clinical *P. aeruginosa* genotypes.

P. aeruginosa is a ubiquitous pathogen capable of causing a wide array of acute and chronic infections. The species is notorious for its unusually large (ca. 6.4 Mbp) genome and extraordinarily diverse genotypes (Silby et al., 2011). As a result, genetic tools established in the model strains, such as PAO1 and PA14, are often inapplicable in the clinical, environmental, and biotechnological strains of interest. Moreover, clinical MDR clones often contain a complex set of resistance markers originating from both chromosomal gene mutations and transferable elements (Cabot et al., 2012; Hocquet et al., 2003), further limiting the conventional antibiotic-resistance-marker-based genetic manipulations. On the other hand, studies have indicated that the genetic background of resistant strains and epistasis among different resistant mutations plays an important role in the resistance levels of the strains and affects the effectiveness of antibiotic chemotherapies (Moura de Sousa et al., 2017; Vogwill et al., 2014, 2016). Hence, it is highly desirable to develop genome-editing techniques compatible with the genotypes of the strains of interests and to characterize AMR in the native genetic background of clinical strains.

In addition to being recognized as a prototypical MDR pathogen, *P. aeruginosa* is also an important model organism for understating CRISPR-Cas functions, especially the most widespread type I CRISPR-Cas system (van Belkum et al., 2015). To exert its functions in the adaptive immune process in bacteria, the Cas proteins specifically bind to and cleave the invader DNA

based on Watson-Crick base pairing between a small CRISPR RNA (crRNA) and its DNA target (Barrangou et al., 2007; Hille et al., 2018). Conceivably, by modifying the sequence of the RNA guide, the Cas nucleases can be reprogrammed to cleave a specific genomic site and be exploited for genome editing upon a repair template is provided (Jinek et al., 2012). Phylogenetic analysis has revealed that CRISPR-Cas systems are widely distributed in global AMR *P. aeruginosa* isolates with ~70% of them belonging to the I-F subtype (van Belkum et al., 2015). In recent years, repurposing the broadly distributed native CRISPR-Cas systems is emerging as a new CRISPR-based genome-editing strategy in prokaryotes. For instance, the native type I-B CRISPR-Cas system was harnessed for genome editing in the medically and industrially important species *Clostridium tyrobutyricum* and *Clostridium pasteurianum*, which frequently suffer from a poor DNA homeostasis and have a low genome-editing efficiency using the traditional allelic exchange or the heterologous CRISPR-Cas9 system (Pyne et al., 2016; Zhang et al., 2018). The endogenous type I-E CRISPR-Cas system was successfully repurposed for genome editing in the commensal bacterium *Lactobacillus crispatus*, which was formerly genetically recalcitrant (Hidalgo-Cantabrana et al., 2019). However, there has been no report about exploitation of native CRISPR-Cas systems for genome editing and functional genomics in the prototypic pathogen *P. aeruginosa*.

Previously, we have isolated an epidemic MDR *P. aeruginosa* clinical strain, PA154197, that shares a clonal complex with two international cystic fibrosis (CF) isolates and displays a comparable resistance profile to the high-risk clone ST175 (Cao et al., 2019). Employing the allelic exchange and the heterologous CRISPR-Cas9-based method failed to deliver desired mutations for resistance characterizations in this strain. As in the majority of clinical and environmental isolates of *P. aeruginosa*, PA154197 is found to contain a native type I-F CRISPR-Cas loci. Hence, in this study, we use PA154197 as a model to explore the native type I-F CRISPR-Cas-based genome editing in a clinical MDR *P. aeruginosa* genotype and its exploitation in the functional genomics of MDR. A highly efficient, one-step (for non-essential gene allele) or two-step insert-delete (In-Del) (for essential gene allele or inefficiently targeted genome site) genome-editing technique was successfully developed. The editing pipeline was readily applicable in additional clinical and environmental *P. aeruginosa* strains tested that contain the endogenous type I-F CRISPR-Cas system. Employing the technique, we unveiled the extraordinary resistance capacity of PA154197 and developed an advanced treatment strategy against this clinical MDR isolate. These studies provided a framework for understanding and control of clinical resistant pathogens.

RESULTS

Functionality of the Native Type I-F CRISPR-Cas Locus in PA154197

Analysis of the CRISPR loci in PA154197 identified the signature *cas8f* gene and the unique *cas2-cas3* fusion (Figure 1A) (Richter et al., 2012), indicating that the loci encode a typical type I-F CRISPR-Cas system. The *cas* operon of the system was found to be sandwiched by two convergent CRISPR arrays with 4 and 10 spacers, respectively. Their consensus repeat sequence differs by only one nucleotide, and their spacers are nearly identical in size (32 bp) (Figure 1A). In addition, a number of spacers show significant homology to phage or putative prophage sequences (data not shown), implying the adaptive immune activity of the endogenous CRISPR-Cas system.

To harness the system for genome editing, we first assessed its genome-targeting activity. We selected *mexB* as the target gene for this purpose, which encodes the inner-membrane component of the housekeeping efflux pump MexAB-OprM. Previous studies have revealed that the canonical target of the type I-F CRISPR-Cas system is 5′-protospacer-GG-3′ with 5′-GG-3′ serving as the protospacer adjacent motif (PAM) sequence (Cady et al., 2012; Richter et al., 2014). Noticeably, because the crRNA guides the base pairing with the complement 5′-protospacer-GG-3′ sequence in the target, earlier studies defined 5′-GG-3′ as the PAM. However, it was recently proposed to follow the guide-centric (5′-CC-3′), rather than the target-centric (5′-GG-3′), terminology (Leenay and Beisel, 2017). Therefore, hereafter the PAM is described as 5′-CC-3′. Thus, an internal 32-bp nucleotide preceded by a 5′-CC-3′ PAM corresponding to the C74-C105 region in *mexB* was selected as the target (PAM protospacer). To achieve specific targeting to this genomic region by the native CRISPR-Cas machinery in PA154197 cells, an artificial mini-CRISPR encompassing the selected 32-bp internal sequence flanked by two 28-bp repeats was assembled. To construct a plasmid-based tool enabling expression and delivery of the mini-CRISPR into PA154197 cells, a strong promoter P*tat* (Shah, 2014) was selected to drive the expression of the mini-CRISPR and the expression cassette was cloned into the pMS402 vector upstream of the *lux* genes (Olsen et al., 1982). Along with the kanamycin resistance marker on the vector, this plasmid tool allows an antibiotic-luminescence dual selection of the transformants (Figure 1B). The resulting plasmid pAY5233 is termed the targeting plasmid in the editing method we developed (Figure 1B). Transformation of pAY5233 into PA154197 cells yielded no transformants recovery compared with the high transformation efficiency of the control plasmid pAY5211, which lacks the mini-CRISPR array (Figure 1C), implying the occurrence of the detrimental chromosome cleavage in the pAY5233-containing cells. This result verified that the native CRISPR-Cas system in PA154197 is active to interfere genomic DNA.

Harnessing the Native Type I-F CRISPR-Cas System to Delete the AMR Gene *mexB*

To exploit the system for gene deletion (Δ*mexB* as an example), we then assembled a 1-kb donor sequence consisting of 500-bp upstream and 500-bp downstream homologous arms of *mexB* and inserted it into pAY5233 to yield pAY5235 (Figure 1D), which is termed the editing plasmid in our method. The transformation recovery rate of pAY5235 into PA154197 cells was significantly increased compared to that of the targeting plasmid pAY5233 (Figure 1C), suggesting the occurrence of homologous recombination by the provision of the repair donor. Since the plasmid tool contains a P*tat*-driven *lux* cassette, luminescence was utilized to assist in the screening of positive clones. Eight luminescent

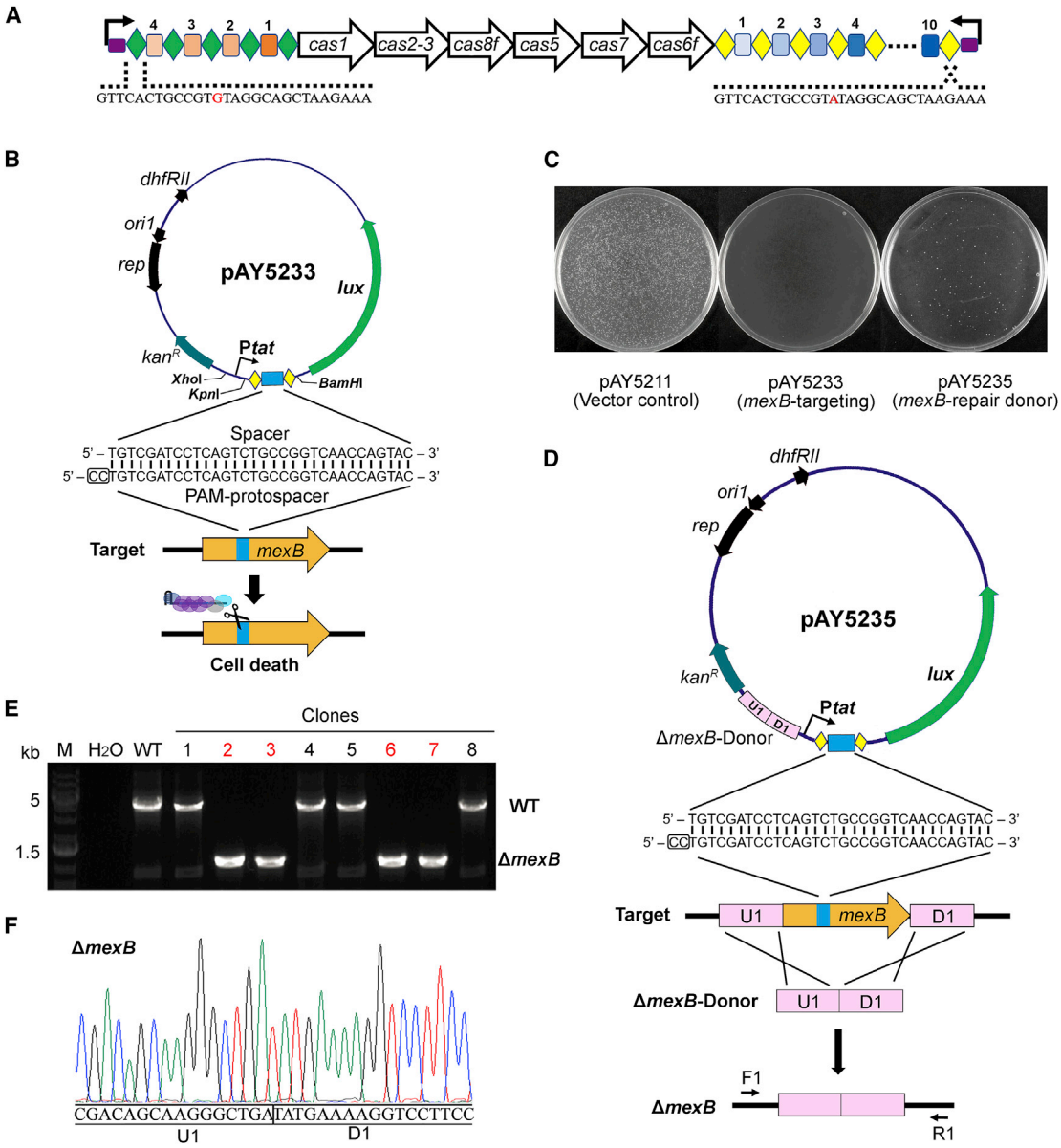

Figure 1. Repurposing the Native Type I-F CRISPR-Cas System for Gene Deletion

(A) Schematic representation of the native type I-F CRISPR-Cas in PA154197. Diamonds and rectangles indicate the repeat and spacer units of a CRISPR array, respectively. Bended arrows (black) above the leader sequence (purple) indicate the orientation of CRISPR transcription. The consensus repeat of the two CRISPR arrays differs by one nucleotide (red).

(B) Schematic showing the design and working mechanism of the *mexB*-targeting plasmid (pAY5233). The mini-CRISPR in pAY5233 comprises a 32-bp spacer (blue) flanked by two repeats (yellow) co-expressed with the reporter *lux* operon (green) under the control of the strong promoter P*tat*. The PAM sequence is framed.

(C) Representative plates showing the transformation efficiency of the vector control pAY5211, the targeting plasmid pAY5233, and the editing plasmid pAY5235.

(D) Design and working mechanism of the editing plasmid pAY5235 containing both a self-targeting CRISPR and a repair donor for *mexB* deletion. The donor sequence (pink) consisting of 500 bp upstream (U1) and downstream (D1) of *mexB* is shown.

(E) Eight randomly selected transformants were subjected to colony PCR to screen for the Δ*mexB* mutants (positive clones are highlighted in red). Primers used in colony PCR (F1/R1) are indicated in (B).

(F) The screened Δ*mexB* mutants in (E) were further validated by DNA sequencing.

See also Figures S1 and S2.

colonies were selected for validation and four colonies showed the desired, scarless, and precise *mexB* deletion (~3 kb) in the chromosome (Figures 1E and 1F).

The success rate increased to more than 90% when the size of the desired gene deletion was decreased to ~1 kb (Figures S1A and S1B), which is the average size of prokaryotic genes

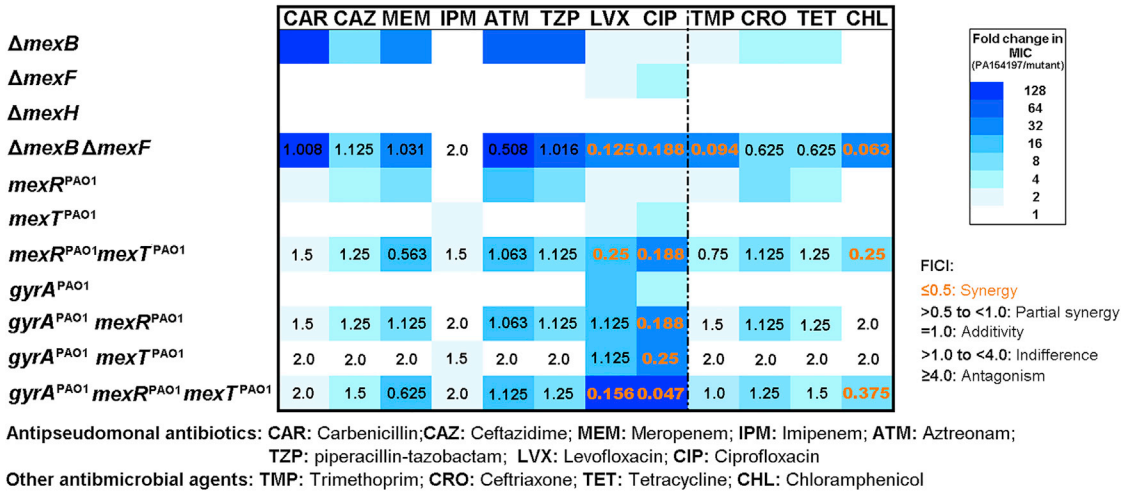

Figure 2. Profile of Antimicrobial Susceptibility Changes Caused by Various Reverse Mutations and Their Synergy Denoted by FICI Values
MICs of 12 antimicrobial agents (8 antipseudomonal antibiotics and 4 other antimicrobial agents) were tested in 12 PA154197 isogenic mutants. MIC fold changes of the mutants relative to the wild-type PA154197 are expressed by the color key shown (detailed MIC values are shown in Table S1). FICI values of various mutation combinations against the antimicrobial agents tested are presented in numbers. FICI values below 0.5 that indicate synergy are highlighted in orange. See also Figure S3 and Tables S1 and S2.

(Xu et al., 2006). Furthermore, the plasmid tool can be readily cured following culturing of the edited cells in the absence of the antibiotic (kanamycin) pressure overnight (Figure S2), suggesting the feasibility of multiple rounds of genome editing using the programmable editing plasmid. Further studies revealed that the technique was readily applicable in two additional type I-F CRISPR-containing clinical and environmental *P. aeruginosa* strains, PA150567 and Ocean-100 (Figure S1C), demonstrating the applicability of the technique in a broad range of *P. aeruginosa* strains isolated from different sources.

Simultaneous Overexpression of the MexAB-OprM and MexEF-OprN Efflux Pumps Constitutes the Major Resistant Determinants in PA154197

Employing the established genetic-editing technique, we first constructed Δ*mexB*, Δ*mexF*, and Δ*mexH* mutants and examined the contribution of three multidrug efflux pumps MexAB-OprM, MexEF-OprN, and MexGHI-OpmD to the resistance profile of PA154197, which were shown to be overexpressed by transcriptome analysis (Cao et al., 2019). Δ*mexB* led to a downshift of minimum inhibitory concentrations (MICs) of all antipseudomonal antibiotics tested (Figure 2; Table S1) with greater fold changes occurring to the antipseudomonal β-lactams and penicillin-β-lactamase inhibitor combinations, i.e., CAR (> 128-fold), CAZ (8-fold), MEM (> 32-fold), ATM (64-fold decrease), TZP (64-fold), than to the fluoroquinolones LVX (2-fold) and CIP (2-fold). Δ*mexF* led to downshift of MICs of antipseudomonal fluoroquinolones (FQs), i.e., LVX (2-fold) and CIP (4-fold), which is consistent with the substrates profile of the two pumps revealed by ectopic overexpression of the genes in laboratory strain PAO1 (Köhler et al., 1997). Unexpectedly, deletion of *mexH* did not lead to any detectable difference in the MICs of all the antibiotics and antimicrobial agents tested (Figure 2; Table S1). Further deletion of *mexH* in the Δ*mexB* Δ*mexF* strain background showed no change on MIC either (data not shown), suggesting that the MexGHI-OpmD pump does not contribute to the resistance development in PA154197.

We further constructed Δ*mexB* Δ*mexF* double deletion to investigate the additive effect of the two pumps, if any. MICs of antipseudomonal β-lactams in the double-deletion strain were similar to those in the Δ*mexB* single-deletion strain, suggesting that β-lactam resistance was largely caused by the MexAB-OprM pump in PA154197. Remarkably, MICs of antipseudomonal FQs were found to be dramatically decreased in the double-deletion cells compared to those in the Δ*mexB* and Δ*mexF* single-deletion cells (Table S1). The MIC fold change of the two FQs (32-fold) was much greater than the multiply of the MIC fold change caused by Δ*mexB* (2-fold) and of Δ*mexF* (2–4-fold) alone, suggesting the synergy of the two pumps to expel fluoroquinolones. We next assessed the synergy by calculating the fractional inhibitory concentration index (FICI) (Gonzales et al., 2015) of the Δ*mexB* Δ*mexF* combination against the antibiotics tested (Figure 2). The FICI value < 0.5 indicates obvious synergy; a FICI value of 0.5–1.0 indicates partial synergy and a FICI value of 1.0–4.0 indicates indifference. The FICI values of the Δ*mexB* Δ*mexF* combination against LVX and CIP were found to be 0.125 and 0.188, respectively, suggesting substantial synergy of the two pumps to expel FQs (Figure 2). Disk diffusion testing showed the similar trend of susceptibility changes in these mutant strains (Figures S3A and S3B). Analysis of growth curves of these strains in the absence of antibiotics suggested that the observed MIC alterations were not caused by growth differences (Figure S3C).

A Two-Step In-Del Strategy to Edit the Essential Gene *gyrA* Reveals the Third Fluoroquinolone Resistance Determinant in PA154197

Although the Δ*mexB* Δ*mexF* double deletion led to a 32-fold downshift of the MICs of LVX (32–1) and CIP (16–0.5), their values

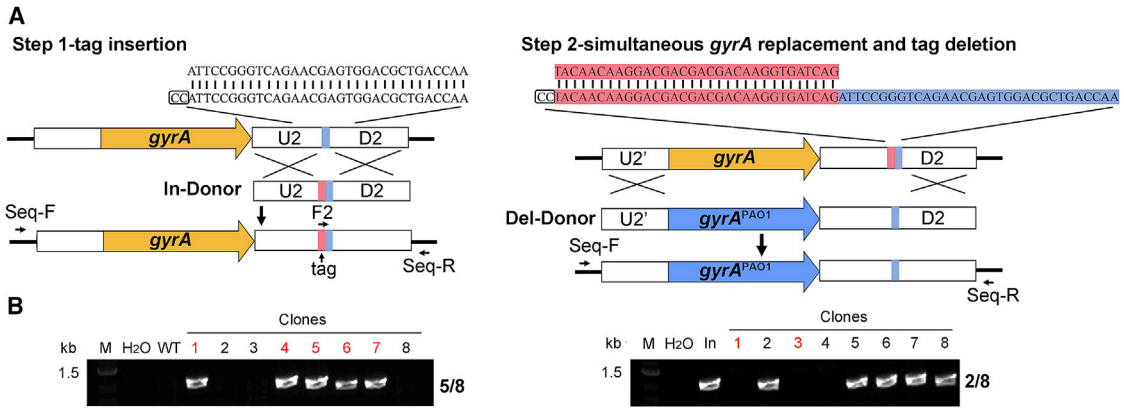

Figure 3. Development of a Two-Step In-Del Approach to Conduct Gene Replacement (*gyrA*^{PAO1}) in an Essential Allele

(A) Schematic showing the two-step In-Del strategy for *gyrA* gene (orange) replacement. A short tag (pink) is first introduced downstream of *gyrA* between the PAM and protospacer portions of a selected target (blue). In the second step, a tag-targeting plasmid carrying the repair donor (Del-donor) is provided. The Del-donor lacks the tag sequence but contains the desired *gyrA*^{PAO1} sequence, which is flanked by two ~1000-bp homologous arms upstream and downstream of the *gyrA* gene. The primer pairs F2/Seq-R and Seq-F/Seq-R were used for the colony PCR analysis and DNA sequencing, respectively.

(B) Eight luminescent positive transformants from each editing step were randomly selected for colony PCR analysis. Desired mutants confirmed by DNA sequencing are highlighted in red.

See also Figured S4 and S5.

in this mutant are still higher than in the control strain PAO1 (MIC of both LVX and CIP is 0.25), suggesting the presence of additional FQ resistance determinants in PA154197. A T248C substitution (corresponding to T83I) in the quinolone resistance determining region (QRDR) (Varughese et al., 2018) of the DNA gyrase gene *gyrA* was identified in PA154197 (Figure S4A). To examine whether this mutation confers further FQ resistance in PA154197, we set out to replace the *gyrA* gene with that in PAO1, i.e., to construct PA154197 *gyrA*^{PAO1}. Since *gyrA* is an essential gene that could not be interfered, we employed an auxiliary PAM located 475 bp downstream of *gyrA* as the target and developed a two-step In-Del strategy to edit this allele (Figure 3). Exploiting the auxiliary PAM, we conducted the first round of editing to insert a 32-bp short tag between the PAM and the protospacer. *gyrA* gene replacement was achieved subsequently in the second round of editing when the short tag was deleted by using the same PAM as in the first step but with a different protospacer sequence (the tag). This time, a donor sequence lacking the tag but containing the desired PAO1 *gyrA* gene sequence was provided to achieve the gene replacement (Figure 3). MICs of LVX and CIP in the resulting strain *gyrA*^{PAO1} were 8- and 4-fold lower than in the PA154197 parent (Figure 2; Table S1), suggesting that *gyrA* mutation indeed contributes to the FQ resistance in PA154197.

Mutations in *mexR* and *mexT* Lead to Simultaneous Overexpression of the *mexAB-oprM* and *mexEF-oprN* Efflux Genes

Overexpression of efflux genes is often caused by mutations in their transcription regulators (Figure 4A). To examine whether a single nucleotide substitution G226T in the transcription repressor gene *mexR* identified in PA154197 (Figure S4B) is responsible for the overexpression of *mexAB-oprM*, we constructed the reverse point mutation *mexR* T226G, which was designated as *mexR*^{PAO1}. The transcriptional level of *mexAB* genes in the *mexR*^{PAO1} mutant was reduced to a similar level to PAO1 (Figure 4B), suggesting that the G226T mutation in *mexR* that introduced a stop codon into MexR following the E76 residue accounts for the overexpression of *mexAB-oprM* in PA154197. Both MIC analysis and the disk diffusion test confirmed this result (Figure S3; Table S1).

The *mexT* gene encodes a transcription activator of the *mexEF-oprN* efflux system (Figure 4A) (Köhler et al., 1999). An 8-bp deletion in *mexT* that was previously described as an *nfxC* type resistant mutation (Linares et al., 2005; Maseda et al., 2000) is identified in PA154197 (Figure S4C). We then employed the two-step In-Del strategy described above to construct the reverse mutation of 8-bp insertion because the nucleotides sequence of the PAM protospacer for the desired editing site in *mexT* contains two 6-bp repeats, which occluded efficient CRISPR recognition and caused failure of DNA interference (Figures S5A and S5B). The resulting mutant was designated as *mexT*^{PAO1}. Both transcription of *mexEF* (Figure 4C) and the MICs of LVX and CIP in the *mexT*^{PAO1} cells were reduced compared to the wild-type (WT) PA154197 (Table S1), indicating that the *nfxC* type 8-bp deletion in *mexT* is responsible for the overexpression of *mexEF-oprN*. Notably, in several non-MDR genotypes, overexpression of the MexEF-OprN pump by MexT in the *nfxC* type *P. aeruginosa* was reported to lead to antagonistic impairment of the MexAB-OprM pump and a hyper-susceptibility to its substrates β-lactams (Figure 4A) (Maseda et al., 2004; Mulet et al., 2011). The fact that the *nfxC* type mutation-containing PA154197 cells over-produce the MexAB-OprM pump and are resistant to β-lactams suggests that either the *mexR* G226T mutation or additional compensatory mutation in PA154197 suppressed the MexT-mediated repression of MexAB-OprM (Figure 4A).

Consistent with its role of simultaneously repressing another AMR gene *oprD* that encodes an outer-membrane (OM) porin protein (Figure 4A), the reverse mutation *mexT*^{PAO1}

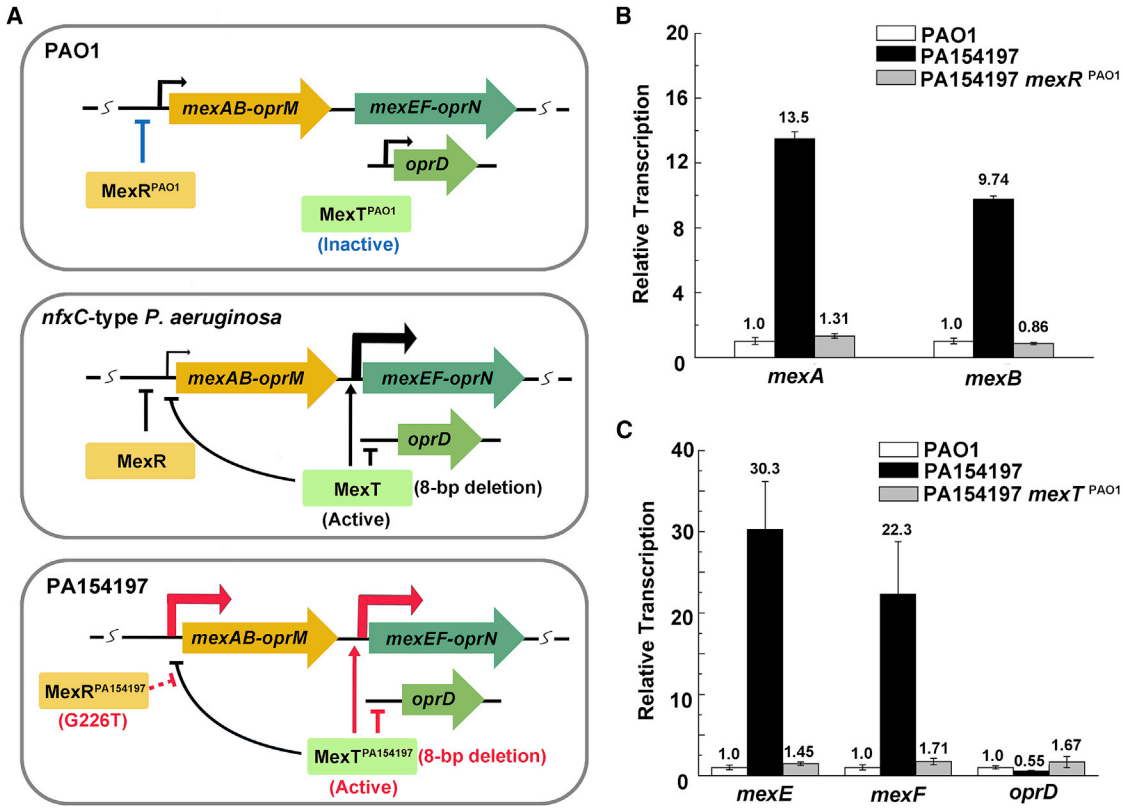

Figure 4. Mutations in *mexR* and *mexT* Lead to Simultaneous Overexpression of the *mexAB-oprM* and *mexEF-oprN* Efflux Pumps

(A) Schematic showing the regulation of *mexAB-oprM*, *mexEF-oprN*, and *oprD* in *P. aeruginosa* PAO1, *nfxC* type mutant, and PA154197. Arrows indicate activation, T-shaped arrows indicate repression, dashed T-shaped arrow indicates potential suppression, and bended arrows with different weights upstream of the genes indicate the relative expression levels of the genes in the three cell backgrounds.

(B) Relative expression of *mexA* and *mexB* in PA154197 and in PAO1, and in PA154197 and its isogenic *mexR*^{PAO1} mutant measured by qRT-PCR.

(C) Relative expression of *mexE*, *mexF*, and *oprD* in PA154197 and in PAO1, and in PA154197 and its isogenic *mexT*^{PAO1} mutant measured by qRT-PCR. Data are represented as the mean ± SD (n = 3).

See also Figure S4.

also led to a 3-fold-higher transcription of *oprD* than the PA154197 parent (Figure 4C) and a restored susceptibility to imipenem (IPM), whose entry is dependent on the OprD portal (Figure S3). In the case of another AMR gene, *parS*, that was proposed to also regulate *mexEF-oprN* system (Wang et al., 2013), reverse mutation of a nonsynonymous nucleotide substitution, G1193A, in the gene (Cao et al., 2019) did not lead to any susceptibility changes to various antibiotics (Table S1), suggesting that this mutation does not contribute to the resistance development in PA154197.

Extensive Resistance Synergy and Multiplication Networks Shape the Clinically Significant MDR in PA154197

We next constructed a series of double- and triple-reverse mutations and examined the interplay of the different resistance determinants. Reverse of all three resistance mutations identified (i.e., *gyrA*^{PAO1}, *mexR*^{PAO1}, and *mexT*^{PAO1}) led to the complete loss of antibiotics resistance and an overall drug susceptibility profile similar to that of PAO1 (Figure 2; Table S1), confirming that these three genetic mutations underlie the resistance development in PA154197. FICI values of the *gyrA*^{PAO1}-*mexR*^{PAO1}-*mexT*^{PAO1} triple combination against the LVX and CIP were calculated to be 0.156 and 0.047, respectively (Figure 2), indicating substantial and extensive synergy of all three determinants to confer the hyper FQ resistance in PA154197. FICI values of the series of reverse-mutation combinations against several non-antipseudomonal antibiotics revealed the strong synergy of overproduction of the two pumps to confer TMP (FICI = 0.094) and CHL (FICI = 0.063) resistance as well and partial synergy toward CRO (FICI = 0.625) and TET (FICI = 0.625) resistance in PA154197.

On the other hand, resistance to antipseudomonal β-lactams including the penicillin-β-lactamase inhibitor combination was almost exclusively dependent on the activity of the MexAB-OprM pump in PA154197. The series of isogenic reverse mutants constructed allowed assessing the relative contribution of basal-level MexAB-OprM and MexAB-OprM over-production to the β-lactams resistance, which can be calculated with the formulas $MIC_{mexR}^{PAO1}/MIC_{\Delta mexB}$ and $MIC_{WT}/MIC_{mexR}^{PAO1}$, respectively. The results suggested that resistance to the antipseudomonal penicillin CAR was largely conferred by basal-level

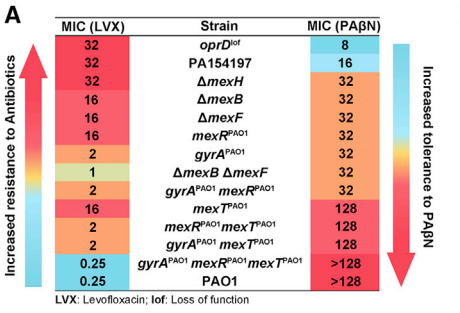

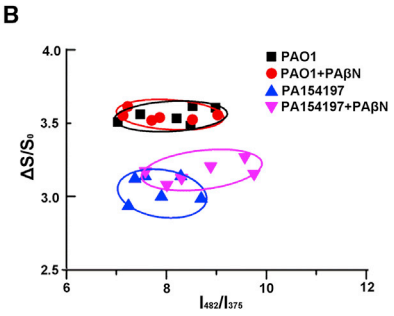

Figure 5. PA154197 Exhibits Collateral Sensitivity to PAβN

(A) Sequential acquisition of antibiotic resistance (LVX as an example) leads to collateral sensitivity to PAβN in PA154197. MICs (μg/ml) of PAO1, PA154197, and a series of isogenic mutants to LVX and PAβN are shown. The relative resistance or tolerance level of the strains to LVX and PAβN is depicted by the color scheme.

(B) 2D graph plotted from output signals of two channels of the PI-BactD sensor: fluorescence increase ($\Delta S/S_0$) and fluorescence ratiometric changes (I_{482}/I_{375}) in each of the strains and treatment indicated. Each assay was conducted in six replicates.

See also Tables S3 and S5.

MexAB-OprM (64-fold MIC change by basal-level pump versus 2-fold by over-produced pump) (Table S2), whereas resistance to the monobactam ATM was largely contributed by the over-production of the MexAB-OprM pump (16- versus 4-fold) (Table S2). The FQ resistance conferred by the MexAB-OprM pump was also attributed to the over-production of the pump (Table S2). Together, these results illustrated the robust interplay among the various types and levels of resistance determinants in PA154197 to confer clinically significant MDR.

PA154197 Displays Collateral Sensitivity to Small Cationic Peptidomimetics in a *mexT*-Dependent Manner

MDR represents the major obstacle in the therapeutics of *P. aeruginosa* infections. To combat drug-resistant infections, it is necessary to both develop new antibiotics and to potentiate the existing antibiotics and preserve the current antibiotics pipeline. Fortuitously, when we attempted to employ the efflux pump inhibitor phenyl-arginine-beta-naphthylamide (PAβN) to treat PA154197, we found that the strain is fairly sensitive to this compound with a MIC value of 16 (μg/ml) (Figure 5A), much lower than the working concentration of the compound (50 μg/ml) to inhibit the basal-level efflux activity (Lamers et al., 2013). Importantly, we found that PA154197 displays a much higher PAβN susceptibility than the control strain PAO1 (MIC > 128). Further analysis of the series of isogenic mutants that reversed one, two, or all three key resistant determinants revealed that their PAβN susceptibilities were intermediate (MIC = 32–128) compared with the PA154197 parent and the reference strain PAO1. The PAβN susceptibility profile of these strains was opposite of that of antibiotics (Figure 5A), indicating that stepwise acquisition of resistance mutations against antibiotics rendered PA154197 susceptible to PAβN. This pattern reflected a phenomenon called "collateral sensitivity," i.e., evolved resistance is costly and resistance mutations to one class of antibiotics may exacerbate susceptibility against other antibiotics or agents (Szybalski and Bryson, 1952). Despite being verified in a series of laboratory-evolved resistant strains of *E. coli* and *P. aeruginosa* (Barbosa et al., 2017; Gonzales et al., 2015; Lázár et al., 2018; Pál et al., 2015; Podnecky et al., 2018; Wambaugh et al., 2017), no systematic investigation and collateral sensitivity has been reported in clinical MDR strains. Our data above indicated that PA154197 displayed collateral sensitivity to PAβN. To further investigate this, we also measured the MICs of other classes of antibiotics including aminoglycosides (streptomycin and gentamycin), non-ribosomal peptides (Polymyxin B and colistin), fosfomycin, and the antimicrobial peptide GF-17 against these strains, but found none of them displayed collateral effects against PA154197 (Table S1).

Furthermore, we found that the collateral effect of PAβN against PA154197 is dependent on the *mexT* gene, as replacing the *mexT* allele with the PAO1 *mexT* (*mexT*^{PAO1}) abolished the susceptibility of PA154197 to PAβN (Figure 5A). Similar abolishment of the collateral sensitivity was observed in all mutants containing *mexT*^{PAO1} (Figure 5A). Notably, this effect is independent of the capacity of MexT to activate the *mexEF-oprN* efflux pump as neither Δ*mexF* nor Δ*mexB* Δ*mexF* double deletion abolished the sensitivity of the strain to PAβN. Since MexT also regulates the OM porin gene *oprD* and PAβN was indicated to also act on the *P. aeruginosa* OM to increase its permeability (Lamers et al., 2013), we speculated that the *mexT*-dependent collateral sensitivity in PA154197 is due to its altered OM features relative to PAO1. To address this, we employed an OM-sensitive probe PI-BactD (Long et al., 2019) to monitor the OM features of PA154197 and PAO1 cells and the cells treated by PAβN. Signals corresponding to PA154197 and PAO1 cells were distinctive in the 2D output graph of the sensor (Figure 5B), suggesting the different physical chemical features of their OM. Furthermore, an obvious signal shift was recorded in the PA154197 population upon PAβN treatment, whereas no signal shift was observed in the PAO1 population in response to the same PAβN treatment (Figure 5B), confirming that the higher susceptibility of PA154197 to PAβN compared to PAO1 was due to the higher susceptibility of its OM to the perturbation by PAβN. Consistent with this, an insertion mutation in the porin gene *oprD* that potentially perturbs the OM of PA154197 cells further increased the sensitivity of the resulting cells to PAβN (MIC = 8) (Figure 5A). Furthermore, sub-inhibitory concentration of PAβN (7.5 μg/ml) was sufficient to sensitize PA154197 to the bulky, anti-Gram-positive antibiotic vancomycin (MIC = 2) (Table S3), which normally is incapable of crossing the OM of Gram-negative bacteria due to the membrane permeability barrier and hence is inactive to Gram-negative cells. Supplement of Mg^{2+}, which stabilizes the OM, reversed this effect, i.e., restored resistance to vancomycin (Table S3).

To further confirm the hyper-sensitivity of PA154197 to small, cationic compounds, we tested and compared the

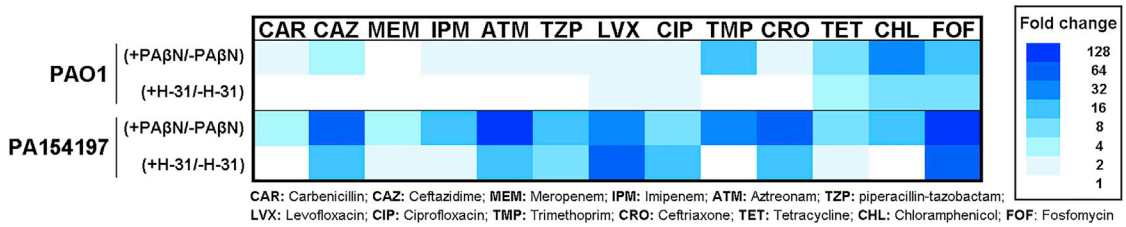

Figure 6. Potentiation Effect of PAβN and H-31 on Various Antibiotics against PA154197 and PAO1

MICs of 13 antimicrobial agents (8 antipseudomonal antibiotics and 5 other antimicrobial agents) were tested in PAO1 and PA154197 in the presence and absence of PAβN (7.5 μg/ml) and H-31 (2 μg/ml), respectively. MIC fold changes following PAβN and H-31 supplementation in the PAO1 and PA154197 cells are denoted by the blue color key. Detailed MIC values in the strains and conditions are shown in Table S4.

sensitivity of PA154197 and PAO1 to another cationic peptidomimetic we developed: (R)-N-(4-(tert-butyl)thiazol-2-yl)-2-chloro-5-(2,6-diaminohexanamido) benzamide (H-31) (Yamaguchi et al., 2017). PA154197 indeed displayed 32-fold lower MIC to H-31 than PAO1 (Table S3). Likewise, sub-inhibitory concentration of H-31 (2 μg/ml) was sufficient to sensitize PA154197 to vancomycin and Mg^{2+} abolished this effect. These results together strongly indicated that acquisition of drug resistance in PA154197 rendered the collateral sensitivity of the cells to small, cationic peptidomimetics due to OM perturbation.

PAβN and H-31 Potentiate Antipseudomonal Antibiotics against the MDR Strain PA154197

We next exploited the identified collateral effect to treat the clinical MDR strain PA154197. We first examined the MICs of various antibiotics against PA154197 in the presence of sub-inhibitory concentration of PAβN (7.5 μg/ml) and H-31 (2 μg/ml), respectively. Supplementing PAβN and H-31 led to 4–128- and 1–64-fold downshifts of MICs of all the antibiotics tested, respectively, demonstrating that PAβN and H-31 potentiates the activities of antibiotics against PA154197 (Figure 6; Table S4). Supplementing the same concentration of PAβN and H-31 also led to the downshift of MICs of these antibiotics against the susceptible strain PAO1, but to a much smaller extent, i.e., 1–8-fold (Figure 6; Table S4). Introduction of $mexT^{PAO1}$ alleviated the antibiotics potentiation effect of PAβN and H-31 against PA154197 (Table S5), further confirming the collateral effect of PAβN and H-31 against PA154197 and its genetic dependence on the *mexT* allele. The sensitivity curve showed that supplementing PAβN and H-31 rendered the MDR PA154197 cells susceptible to antibiotics, such as IPM and FOF, and the susceptibility was greater than the PAO1 cells (Figure 7). To further examine the efficacy of collateral agents and antibiotics combinations against the MDR *P. aeruginosa* cells, we co-administrated 7.5 μg/ml PAβN or 2 μg/ml H-31 with two antibiotics, 4MIC IPM and 4MIC FOF, to PA154197 or PAO1 cell cultures and analyzed their killing kinetics. The combined treatment not only was more effective against the MDR strain PA154197 than against the susceptible strain PAO1 but also displayed an accelerated killing against PA154197 than against PAO1 (Figure S6), demonstrating the applicability of the uncovered collateral sensitivity in anti-resistance interventions against clinical MDR strains.

DISCUSSION

Due to the difficulty of genetic manipulation in the clinical isolates of resistant pathogens, understanding of their resistance development has been largely based on comparative genomics and heterologous reconstitution in the laboratory model strains (Jia et al., 2017). In this study, we established a single-plasmid-mediated, highly efficient genome-editing technique in the prototypic pathogen *P. aeruginosa* by harnessing the most common CRISPR-Cas system (type I-F) in the species. Compared with a recently reported heterologous Cas9-based genome-editing method in *P. aeruginosa* model strains that requires successive transformation of two editing plasmids (Chen et al., 2018), and the conventional two-step allelic exchange method (Choi and Schweizer, 2005), which is more laborious and results in an undesirable flippase recognition target (*FRT*) scar in the edited site, our method of using a one-step transformation of a single editing plasmid represents a more efficient and cleaner genome-editing technique, especially in those clinical and environmental strains suffering a poor DNA homeostasis. Combined with the two-step In-Del strategy, this technique enabled various non-lethal genetic manipulations in *P. aeruginosa* cells.

Employing this powerful editing technique, not only the key resistant determinants but also their synergy and multiplication networks underling the extraordinary antibiotic recalcitrance of PA154197 were identified. Two RND efflux pumps, MexAB-OprM and MexEF-OprN, are simultaneously over-produced and synergize the efflux of FQs, CHL, and TMP in PA154197. Interestingly, previous studies using genetic reconstitution in laboratory strains suggested that there is a lack of multiplicative or synergetic effects between over-expression of multidrug efflux pumps (Bruchmann et al., 2013; Horna et al., 2018; Köhler et al., 1999; Li et al., 2015; Llanes et al., 2004; Riera et al., 2011). Particularly, in the *nfxC* type *P. aeruginosa* strains, over-production of MexEF-OprN was found to be antagonistic to the MexAB-OprM pump. (Maseda et al., 2004; Mulet et al., 2011). These results together suggested that clinical MDR *P. aeruginosa* strains might have developed compensatory mutations to overcome the fitness trade-off of overexpressing more than one of the efflux pumps, which warrants further investigations in the future.

Despite its increasing therapeutic implications in the treatment of drug-resistant pathogens (Barbosa et al., 2017; Lázár et al., 2018; Pál et al., 2015; Podnecky et al., 2018; Szybalski and

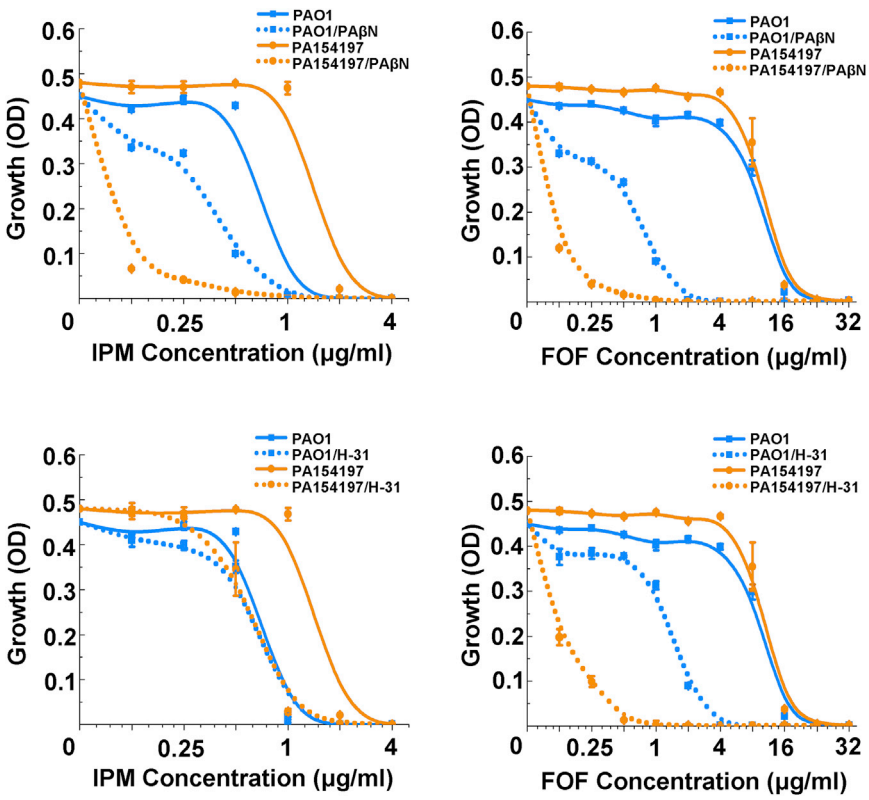

Figure 7. PAβN and H-31 Dramatically Increases the Sensitivity of PA154197 to Imipenem (IPM) and Fosfomycin (FOF)

MIC assays for IPM (left) and FOF (right) sensitivity in PAO1 and PA154197 with or without the supplement of PAβN (7.5 μg/ml, upper) or H-31 (2 μg/ml, bottom). Data are represented as the mean ± SD (n = 3). See also Figure S6 and Table S4.

Bryson, 1952; Wambaugh et al., 2017), research about collateral sensitivity has largely focused on the laboratory-evolved strain lines that display resistance to specific classes of antibiotics, and little effort has focused on the clinically isolated MDR strains (Imamovic et al., 2018; Jansen et al., 2016). The series of constructed isogenic mutants that mimic the sequential acquisition of the key resistance mutations enabled us to identify the collateral sensitivity of PA154197 to small cationic peptidomimetics due to its compromised OM permeability. Interestingly, a recent study on a set of 60 laboratory-evolved antibiotic-resistant *E. coli* also revealed a widespread collateral sensitivity of the resistant strains to the OM targeting agent antimicrobial peptides (Lázár et al., 2018), suggesting that OM perturbation caused by resistance mutations may represent a common mechanism of collateral sensitivity in Gram-negative bacteria. However, unlike the set of 60 AMR *E. coli* strains, PA154197 does not show collateral sensitivity to cationic antimicrobial peptides, such as GF-17, or to cationic peptide antibiotics, such as PMB and CST, which disrupt Gram-negative bacteria OM by their interactions with lipopolysaccharide (LPS) molecules (Wang et al., 2015), suggesting that different types of OM perturbations other than LPS modification occurred in PA154197.

Furthermore, we revealed that *mexT* is the key genetic determinant underlying the collateral sensitivity of PA154197 to small cationic peptidomimetics. Interestingly, a resistance mutation in the transcription regulator *marR* that simultaneously regulates the expression of the *acrAB* multidrug efflux pump gene and LPS modification genes in *E. coli* was found to underlie the collateral sensitivity of the cells to antimicrobial peptides (Lázár et al., 2018). Analogously, in addition to regulating the *mexEF* multidrug efflux pump, MexT is known to also regulate the porin gene *oprD* and a series of other genes in *P. aeruginosa* (Tian et al., 2009). These results suggested that transcription regulators that simultaneously regulate membrane-associated resistance determinants and other membrane homeostasis genes may represent as the common genetic determinants of collateral sensitivity. These findings have important implications in characterizing collateral sensitivity in other Gram-negative resistant pathogens.

Lastly, we found that overexpression (~40-fold higher than in PAO1) of the efflux gene *mexH* and nucleotide substitution in *parS* did not contribute to the drug resistance in PA154197. These results suggest that not all genetic variations in resistance genes lead to the development of antibiotic resistance phenotypes, further highlighting the importance and necessity of the targeted functional genomics in the genetic background of clinically resistant pathogens.

STAR★METHODS

Detailed methods are provided in the online version of this paper and include the following:

- KEY RESOURCES TABLE
- LEAD CONTACT AND MATERIALS AVAILABILITY
- EXPERIMENTAL MODEL AND SUBJECT DETAILS
- METHOD DETAILS
  - Plasmid Construction
  - Transformation of PA154197
  - Mutants Screening and Verification
  - Curing of Editing Plasmid
  - Antibiotic Sensitivity Assays
  - Quantitative reverse transcriptase PCR
  - Disk Diffusion Assay
  - Fractional Inhibitory Concentration Index
  - PI-BactD Assay
  - Time-Kill Assay
- QUANTIFICATION AND STATISTICAL ANALYSIS
- DATA AND CODE AVAILABILITY

SUPPLEMENTAL INFORMATION

Supplemental Information can be found online at https://doi.org/10.1016/j.celrep.2019.10.006.

ACKNOWLEDGMENTS

We thank Prof. Susumu Yoshizawa and Prof. Kazuhiro Kogure (both from the University of Tokyo) for sharing the ocean-100 strain. We thank Prof. Xuechen Li (Department of Chemistry, The University of Hong Kong) for providing the GF-17 peptide and Dr. Xin Deng (Department of Biomedical Sciences, City University of Hong Kong) for the pMS402 vector. We thank Dr. Zhaoxun Liang (School of Biological Sciences, Nanyang Technological University, Singapore) for his stimulating discussion with us about the manuscript, and Prof. Min Wu (School of Medicine and Health Sciences, University of North Dakota) for proofreading the manuscript. This work was supported by the Hong Kong University Grants Council General Research Fund (HKU17142316 to A.Y.); the Seed Funding for Basic Research Scheme of The University of Hong Kong (201711159278 to A.Y.); the Seed Funding for Strategic Interdisciplinary Research Scheme (HKU 2017 to A.Y.); the National Natural Science Foundation of China (No. 31571283 to H.X.); and the National Transgenic Science and Technology Program (2019ZX08010-003 to M.L.).

AUTHOR CONTRIBUTIONS

Z.X., M.L., H.X., and A.Y. designed the research; Z.X. and Y.L. performed the experiments; H.C. contributed to the bioinformatic analysis; L.M. and Z.C.X. synthesized PI-BactD and performed the PI-BactD assay; Y.H., S.Y., and K.N. synthesized and provided H-31; P.C.Y.W. provided clinical PA isolates and participated in the data analysis; and Z.X., M.L., H.X., and A.Y. analyzed the data and wrote the manuscript.

DECLARATION OF INTERESTS

The authors declare no competing interests.

Received: June 2, 2019
Revised: September 9, 2019
Accepted: September 30, 2019
Published: November 5, 2019

REFERENCES

Barbosa, C., Trebosc, V., Kemmer, C., Rosenstiel, P., Beardmore, R., Schulenburg, H., and Jansen, G. (2017). Alternative evolutionary paths to bacterial antibiotic resistance cause distinct collateral effects. Mol. Biol. Evol. *34*, 2229–2244.

Barrangou, R., Fremaux, C., Deveau, H., Richards, M., Boyaval, P., Moineau, S., Romero, D.A., and Horvath, P. (2007). CRISPR provides acquired resistance against viruses in prokaryotes. Science *315*, 1709–1712.

Bruchmann, S., Dötsch, A., Nouri, B., Chaberny, I.F., and Häussler, S. (2013). Quantitative contributions of target alteration and decreased drug accumulation to Pseudomonas aeruginosa fluoroquinolone resistance. Antimicrob. Agents Chemother. *57*, 1361–1368.

Cabot, G., Ocampo-Sosa, A.A., Domínguez, M.A., Gago, J.F., Juan, C., Tubau, F., Rodríguez, C., Moyà, B., Peña, C., Martínez-Martínez, L., and Oliver, A.; Spanish Network for Research in Infectious Diseases (REIPI) (2012). Genetic markers of widespread extensively drug-resistant *Pseudomonas aeruginosa* high-risk clones. Antimicrob. Agents Chemother. *56*, 6349–6357.

Cady, K.C., Bondy-Denomy, J., Heussler, G.E., Davidson, A.R., and O'Toole, G.A. (2012). The CRISPR/Cas adaptive immune system of *Pseudomonas aeruginosa* mediates resistance to naturally occurring and engineered phages. J. Bacteriol. *194*, 5728–5738.

Cao, H., Xia, T., Li, Y., Xu, Z., Bougouffa, S., Lo, Y.K., Bajic, V.B., Luo, H., Woo, P.C.Y., and Yan, A. (2019). Uncoupled quorum sensing modulates the interplay of virulence and resistance in a multidrug-resistant clinical *Pseudomonas aeruginosa* isolate belonging to the MLST550 clonal complex. Antimicrob. Agents Chemother. *63*, e01944-18.

Chen, W., Zhang, Y., Zhang, Y., Pi, Y., Gu, T., Song, L., Wang, Y., and Ji, Q. (2018). CRISPR/Cas9-based genome editing in Pseudomonas aeruginosa and cytidine deaminase-mediated base editing in Pseudomonas species. iScience *6*, 222–231.

Choi, K.H., and Schweizer, H.P. (2005). An improved method for rapid generation of unmarked *Pseudomonas aeruginosa* deletion mutants. BMC Microbiol. *5*, 30.

Gonzales, P.R., Pesesky, M.W., Bouley, R., Ballard, A., Biddy, B.A., Suckow, M.A., Wolter, W.R., Schroeder, V.A., Burnham, C.A.D., Mobashery, S., et al. (2015). Synergistic, collaterally sensitive β-lactam combinations suppress resistance in MRSA. Nat. Chem. Biol. *11*, 855–861.

Hidalgo-Cantabrana, C., Goh, Y.J., Pan, M., Sanozky-Dawes, R., and Barrangou, R. (2019). Genome editing using the endogenous type I CRISPR-Cas system in *Lactobacillus crispatus*. Proc. Natl. Acad. Sci. USA *116*, 15774–15783.

Hille, F., Richter, H., Wong, S.P., Bratovič, M., Ressel, S., and Charpentier, E. (2018). The biology of CRISPR-Cas: backward and forward. Cell *172*, 1239–1259.

Hocquet, D., Bertrand, X., Köhler, T., Talon, D., and Plésiat, P. (2003). Genetic and phenotypic variations of a resistant *Pseudomonas aeruginosa* epidemic clone. Antimicrob. Agents Chemother. *47*, 1887–1894.

Horna, G., López, M., Guerra, H., Saénz, Y., and Ruiz, J. (2018). Interplay between MexAB-OprM and MexEF-OprN in clinical isolates of *Pseudomonas aeruginosa*. Sci. Rep. *8*, 16463.

Imamovic, L., Ellabaan, M.M.H., Dantas Machado, A.M., Citterio, L., Wulff, T., Molin, S., Krogh Johansen, H., and Sommer, M.O.A. (2018). Drug-driven phenotypic convergence supports rational treatment strategies of chronic infections. Cell *172*, 121–134.e14.

Jansen, G., Mahrt, N., Tueffers, L., Barbosa, C., Harjes, M., Adolph, G., Friedrichs, A., Krenz-Weinreich, A., Rosenstiel, P., and Schulenburg, H. (2016). Association between clinical antibiotic resistance and susceptibility of *Pseudomonas* in the cystic fibrosis lung. Evol. Med. Public Health *2016*, 182–194.

Jia, B., Raphenya, A.R., Alcock, B., Waglechner, N., Guo, P., Tsang, K.K., Lago, B.A., Dave, B.M., Pereira, S., Sharma, A.N., et al. (2017). CARD 2017: expansion and model-centric curation of the comprehensive antibiotic resistance database. Nucleic Acids Res. *45* (*D1*), D566–D573.

Jinek, M., Chylinski, K., Fonfara, I., Hauer, M., Doudna, J.A., and Charpentier, E. (2012). A programmable dual-RNA-guided DNA endonuclease in adaptive bacterial immunity. Science *337*, 816–821.

Köhler, T., Michéa-Hamzehpour, M., Henze, U., Gotoh, N., Curty, L.K., and Pechère, J.C. (1997). Characterization of MexE-MexF-OprN, a positively regulated multidrug efflux system of *Pseudomonas aeruginosa*. Mol. Microbiol. *23*, 345–354.

Köhler, T., Epp, S.F., Curty, L.K., and Pechère, J.C. (1999). Characterization of MexT, the regulator of the MexE-MexF-OprN multidrug efflux system of *Pseudomonas aeruginosa*. J. Bacteriol. *181*, 6300–6305.

Kumagai, Y., Yoshizawa, S., Nakamura, K., Ogura, Y., Hayashi, T., and Kogure, K. (2017). Complete and draft genome sequences of eight oceanic *Pseudomonas aeruginosa* strains. Genome Announc. *5*, e01255-17.

Lamers, R.P., Cavallari, J.F., and Burrows, L.L. (2013). The efflux inhibitor phenylalanine-arginine beta-naphthylamide (PAβN) permeabilizes the outer membrane of gram-negative bacteria. PLoS ONE *8*, e60666.

Lázár, V., Martins, A., Spohn, R., Daruka, L., Grézal, G., Fekete, G., Számel, M., Jangir, P.K., Kintses, B., Csörgő, B., et al. (2018). Antibiotic-resistant bacteria show widespread collateral sensitivity to antimicrobial peptides. Nat. Microbiol. *3*, 718–731.

Leenay, R.T., and Beisel, C.L. (2017). Deciphering, communicating, and engineering the CRISPR PAM. J. Mol. Biol. *429*, 177–191.

Li, X.Z., Plésiat, P., and Nikaido, H. (2015). The challenge of efflux-mediated antibiotic resistance in Gram-negative bacteria. Clin. Microbiol. Rev. *28*, 337–418.

Linares, J.F., López, J.A., Camafeita, E., Albar, J.P., Rojo, F., and Martínez, J.L. (2005). Overexpression of the multidrug efflux pumps MexCD-OprJ and MexEF-OprN is associated with a reduction of type III secretion in *Pseudomonas aeruginosa*. J. Bacteriol. *187*, 1384–1391.

Llanes, C., Hocquet, D., Vogne, C., Benali-Baitich, D., Neuwirth, C., and Plésiat, P. (2004). Clinical strains of *Pseudomonas aeruginosa* overproducing MexAB-OprM and MexXY efflux pumps simultaneously. Antimicrob. Agents Chemother. *48*, 1797–1802.

Long, S., Miao, L., Li, R., Deng, F., Qiao, Q., Liu, X., Yan, A., and Xu, Z. (2019). Rapid Identification of Bacteria by Membrane-Responsive Aggregation of a Pyrene Derivative. ACS Sens. *4*, 281–285.

Maseda, H., Saito, K., Nakajima, A., and Nakae, T. (2000). Variation of the *mexT* gene, a regulator of the MexEF-oprN efflux pump expression in wild-type strains of *Pseudomonas aeruginosa*. FEMS Microbiol. Lett. *192*, 107–112.

Maseda, H., Sawada, I., Saito, K., Uchiyama, H., Nakae, T., and Nomura, N. (2004). Enhancement of the *mexAB-oprM* efflux pump expression by a quorum-sensing autoinducer and its cancellation by a regulator, MexT, of the *mexEF-oprN* efflux pump operon in *Pseudomonas aeruginosa*. Antimicrob. Agents Chemother. *48*, 1320–1328.

Mohamed, M.F., Hamed, M.I., Panitch, A., and Seleem, M.N. (2014). Targeting methicillin-resistant *Staphylococcus aureus* with short salt-resistant synthetic peptides. Antimicrob. Agents Chemother. *58*, 4113–4122.

Moura de Sousa, J., Balbontín, R., Durão, P., and Gordo, I. (2017). Multidrug-resistant bacteria compensate for the epistasis between resistances. PLoS Biol. *15*, e2001741.

Mulet, X., Moyá, B., Juan, C., Macià, M.D., Pérez, J.L., Blázquez, J., and Oliver, A. (2011). Antagonistic interactions of *Pseudomonas aeruginosa* antibiotic resistance mechanisms in planktonic but not biofilm growth. Antimicrob. Agents Chemother. *55*, 4560–4568.

Oliver, A., Mulet, X., López-Causapé, C., and Juan, C. (2015). The increasing threat of *Pseudomonas aeruginosa* high-risk clones. Drug Resist. Updat. *21-22*, 41–59.

Olsen, R.H., DeBusscher, G., and McCombie, W.R. (1982). Development of broad-host-range vectors and gene banks: self-cloning of the *Pseudomonas aeruginosa* PAO chromosome. J. Bacteriol. *150*, 60–69.

Pál, C., Papp, B., and Lázár, V. (2015). Collateral sensitivity of antibiotic-resistant microbes. Trends Microbiol. *23*, 401–407.

Podnecky, N.L., Fredheim, E.G.A., Kloos, J., Sørum, V., Primicerio, R., Roberts, A.P., Rozen, D.E., Samuelsen, Ø., and Johnsen, P.J. (2018). Conserved collateral antibiotic susceptibility networks in diverse clinical strains of *Escherichia coli*. Nat. Commun. *9*, 3673.

Poole, K. (2011). *Pseudomonas aeruginosa*: resistance to the max. Front. Microbiol. *2*, 65.

Pyne, M.E., Bruder, M.R., Moo-Young, M., Chung, D.A., and Chou, C.P. (2016). Harnessing heterologous and endogenous CRISPR-Cas machineries for efficient markerless genome editing in *Clostridium*. Sci. Rep. *6*, 25666.

Rankin, I.D. (2005). MIC testing. In Manual of Antimicrobial Susceptibility Testing, M.B. Coyle, ed. (American Society for Microbiology), pp. 53–62.

Richter, C., Gristwood, T., Clulow, J.S., and Fineran, P.C. (2012). In vivo protein interactions and complex formation in the *Pectobacterium atrosepticum* subtype I-F CRISPR/Cas System. PLoS ONE *7*, e49549.

Richter, C., Dy, R.L., McKenzie, R.E., Watson, B.N., Taylor, C., Chang, J.T., McNeil, M.B., Staals, R.H., and Fineran, P.C. (2014). Priming in the Type I-F CRISPR-Cas system triggers strand-independent spacer acquisition, bi-directionally from the primed protospacer. Nucleic Acids Res. *42*, 8516–8526.

Riera, E., Cabot, G., Mulet, X., García-Castillo, M., del Campo, R., Juan, C., Cantón, R., and Oliver, A. (2011). *Pseudomonas aeruginosa* carbapenem resistance mechanisms in Spain: impact on the activity of imipenem, meropenem and doripenem. J. Antimicrob. Chemother. *66*, 2022–2027.

Santajit, S., and Indrawattana, N. (2016). Mechanisms of antimicrobial resistance in ESKAPE pathogens. BioMed Res. Int. *2016*, 2475067.

Shah, N.C.M. (2014). Construction and development of bioluminescent *Pseudomonas aeruginosa* strains; application in biosensors for preservative efficacy testing (University of Hertfordshire Research Archive). https://uhra.herts.ac.uk/handle/2299/15592.

Silby, M.W., Winstanley, C., Godfrey, S.A., Levy, S.B., and Jackson, R.W. (2011). *Pseudomonas* genomes: diverse and adaptable. FEMS Microbiol. Rev. *35*, 652–680.

Stover, C.K., Pham, X.Q., Erwin, A.L., Mizoguchi, S.D., Warrener, P., Hickey, M.J., Brinkman, F.S., Hufnagle, W.O., Kowalik, D.J., Lagrou, M., et al. (2000). Complete genome sequence of *Pseudomonas aeruginosa* PAO1, an opportunistic pathogen. Nature *406*, 959–964.

Szybalski, W., and Bryson, V. (1952). Genetic studies on microbial cross resistance to toxic agents. I. Cross resistance of Escherichia coli to fifteen antibiotics. J. Bacteriol. *64*, 489–499.

Tian, Z.X., Fargier, E., Mac Aogáin, M., Adams, C., Wang, Y.P., and O'Gara, F. (2009). Transcriptome profiling defines a novel regulon modulated by the LysR-type transcriptional regulator MexT in *Pseudomonas aeruginosa*. Nucleic Acids Res. *37*, 7546–7559.

van Belkum, A., Soriaga, L.B., LaFave, M.C., Akella, S., Veyrieras, J.-B., Barbu, E.M., Shortridge, D., Blanc, B., Hannum, G., Zambardi, G., et al. (2015). Phylogenetic distribution of CRISPR-Cas systems in antibiotic-resistant *Pseudomonas aeruginosa*. MBio *6*, e01796–e15.

Varughese, L.R., Rajpoot, M., Goyal, S., Mehra, R., Chhokar, V., and Beniwal, V. (2018). Analytical profiling of mutations in quinolone resistance determining region of *gyrA* gene among UPEC. PLoS ONE *13*, e0190729.

Vogwill, T., Kojadinovic, M., Furió, V., and MacLean, R.C. (2014). Testing the role of genetic background in parallel evolution using the comparative experimental evolution of antibiotic resistance. Mol. Biol. Evol. *31*, 3314–3323.

Vogwill, T., Kojadinovic, M., and MacLean, R.C. (2016). Epistasis between antibiotic resistance mutations and genetic background shape the fitness effect of resistance across species of *Pseudomonas*. Proc. Biol. Sci. *283*, 1830.

Wambaugh, M.A., Shakya, V.P.S., Lewis, A.J., Mulvey, M.A., and Brown, J.C.S. (2017). High-throughput identification and rational design of synergistic small-molecule pairs for combating and bypassing antibiotic resistance. PLoS Biol. *15*, e2001644.

Wang, D., Seeve, C., Pierson, L.S., 3rd, and Pierson, E.A. (2013). Transcriptome profiling reveals links between ParS/ParR, MexEF-OprN, and quorum sensing in the regulation of adaptation and virulence in *Pseudomonas aeruginosa*. BMC Genomics *14*, 618.

Wang, X., Quinn, P.J., and Yan, A. (2015). Kdo2 -lipid A: structural diversity and impact on immunopharmacology. Biol. Rev. Camb. Philos. Soc. *90*, 408–427.

Xu, L., Chen, H., Hu, X., Zhang, R., Zhang, Z., and Luo, Z.W. (2006). Average gene length is highly conserved in prokaryotes and eukaryotes and diverges only between the two kingdoms. Mol. Biol. Evol. *23*, 1107–1108.

Yamaguchi, A., Kato, O., Inoue, Y., Yamazaki, S., Higuchi, Y., Sakurai, K., Nakajima, R., and Nishino, K. (2017). Multiple drug discharge pump inhibitor. Patent JP2017105714 (A), Date filed: 12-07-2015; Date granted: 06-15-2017.

Zhang, J., Zong, W., Hong, W., Zhang, Z.T., and Wang, Y. (2018). Exploiting endogenous CRISPR-Cas system for multiplex genome editing in *Clostridium tyrobutyricum* and engineer the strain for high-level butanol production. Metab. Eng. *47*, 49–59.

STAR★METHODS

KEY RESOURCES TABLE

REAGENT or RESOURCE	SOURCE	IDENTIFIER
Bacterial and Virus Strains		
PA154197	This paper	N/A
PA150567	This paper	N/A
Ocean-100	Kumagai et al., 2017	N/A
DH5α	This paper	N/A
PA154197 mutants, see Table S6	This paper	N/A
Chemicals, Peptides, and Recombinant Proteins		
Phe-Arg β-naphthylamide dihydrochloride (PAβN)	Sigma-Aldrich	Cat#P4157
(R)-N-(4-(tert-butyl)thiazol-2-yl)-2-chloro-5-(2,6-diaminohexanamido) benzamide (H-31)	Yamaguchi et al., 2017	N/A
Critical Commercial Assays		
Quick Ligation™ Kit	New England Biolabs	Cat#M2200
ClonExpress II One Step Cloning Kit	Vazyme	C112
iProof High-Fidelity DNA Polymerase	Bio-Rad	Cat#1725301
Taq DNA polymerase	Thermo Scientific	Cat#EP0406
RNeasy Mini Kit	QIAGEN	Cat#74104
PrimeScript™ RT reagent Kit	Takara	Cat#RR037A
SYBR™ Green PCR master mix	Applied Biosystems	Cat#4344463
Oligonucleotides		
Primer list, see Table S6	This paper	N/A
Recombinant DNA		
Plasmid list, see Table S6	This paper	N/A
Software and Algorithms		
Chromas	Technelysium Pty Ltd	https://technelysium.com.au/wp/chromas/

LEAD CONTACT AND MATERIALS AVAILABILITY

Further information and requests for resources and reagents should be directed to and will be fulfilled by the Lead Contact, Aixin Yan (ayan8@hku.hk). This study did not generate new unique reagents.

EXPERIMENTAL MODEL AND SUBJECT DETAILS

All the bacterial strains used and constructed in this study are listed in Table S6. *E. coli* DH5α is used for plasmid propagation and is usually cultured at 37°C in Luria-Bertani (LB) broth or on the LB agar plate supplemented with 20 μg/ml Kanamycin (KAN). *P. aeruginosa* PA154197 was isolated from the Queen Mary Hospital in Hong Kong, China (Cao et al., 2019). PA154197 and its derivatives were selected on LB agar plate with 500 μg/ml KAN.

METHOD DETAILS

Plasmid Construction

All the plasmids constructed and used in this study are listed in Table S6. Mini-CRISPR element consisting of two repeats (GTTCACTGCCGTATAGGCAGCTAAGAAA) flanking the spacer (Spacer sequence, see Table S6) was synthesized by BGI (Shenzhen, China). PCR was performed using the iProof High-Fidelity DNA Polymerase (Bio-Rad, USA). Mini-CRISPR elements and plasmid pAY5211 were digested using the restriction enzymes KpnI and *BamH*I (NEB, USA) and ligated using the Quick Ligation™ Kit (NEB, USA). Donor sequences which typically contain 500-bp upstream and 500-bp downstream of the editing sites with 21-bp overlap of the *Xho*I-digested targeting plasmid at each end (See Donor-Up-F/Donor-Down-R in Table S6) were amplified by PCR and ligated

into the linearized targeting plasmid (digested by *Xho*I (NEB, USA)) using the ClonExpress II One Step Cloning Kit (Vazyme, China). All the constructed plasmids were verified by DNA sequencing (BGI, China) using primers pMS402-seq-F/pMS402-seq-R (Table S6).

Transformation of PA154197

Electrocompetent PA154197 cells were prepared by inoculating a fresh colony in LB broth and grown at 37°C overnight with 220-rpm agitation. Following subculture (1:100 dilution) into 50 mL fresh LB broth and growing to OD_{600} = 0.5-0.6, cells were collected by centrifugation at 4°C with 4,500 rpm for 15 min and washed three times with cold, autoclaved Milli-Q H_2O. The resulting cells were resuspended into 1 mL Milli-Q H_2O. 100 μL electrocompetent PA154197 cells were then mixed with 1 μg editing plasmid and subject to electroporation at 2.3 kV (BTX, USA). 1 mL cold LB broth was added to recover the cells. Following recovering at 37°C for 1.5 h with agitation, cells were pelleted and resuspended in 100 μL LB before spread onto the LB plates containing 500 μg/ml KAN. The plates were incubated at 37°C for 24 h.

Mutants Screening and Verification

Colonies were first subjected to luminescence screening using the Synergy HTX Plate Reader (Bio Tek, USA). Colonies with high luminescent intensity were further verified by colony PCR using Taq DNA polymerase (Thermal Scientific, USA) with indicated primers and DNA sequencing (BGI, China). Sequencing results were visualized using DNA sequencing software Chromas (Technelysium Pty Ltd, Australia)

Curing of Editing Plasmid

P. aeruginosa cells underwent one round of editing was streaked onto the LB ager plate and incubated at 37°C overnight. Single colony was selected and the curing was verified by the failure of growth in LB broth with 100 μg/ml KAN. In some cases, multiple (2 to 3) rounds of streaking are required for the thorough plasmid curing.

Antibiotic Sensitivity Assays

Minimum inhibitory concentration (MIC) was measured in 96-well plate following the standard protocol of ASM with slight modification (Rankin, 2005). Overnight culture was diluted and approximately 10^5 cells were inoculated in each well containing antibiotic with final concentrations ranging from 0.25 to 128 μg/ml. Following incubation at 37°C for 16-20 h, MIC values were determined as the lowest concentration of antibiotics that completely inhibit growth of bacteria as detected by the unaided eye. Growth measurement shown in Figure 7 was set up in exactly the same manner as the MIC assay, except that cultures were grown at 37°C in the Synergy HTX Plate Reader (Bio Tek, USA) for 12 h with agitation. Cell density (OD_{600}) at 12 h was selected to plot the sensitivity curves. Assays were performed in triplicate.

Quantitative reverse transcriptase PCR

Bacterial cells from overnight culture were harvested by centrifugation at 4°C. Total RNA was extracted using RNeasy Mini Kit (QIAGEN, Germany) according to the manufacturer's instruction. Reverse transcription (RT) was performed using PrimeScript™ RT reagent Kit (Takara, Japan). Quantitative PCR was performed using specific primers and the SYBR™ Green PCR master mix (Applied Biosystems, USA) in a 20 μL reaction system. The reaction was performed in ABI StepOnePlus real time PCR system with *recA* and *clpX* as reference genes to normalize the relative expression of the target genes. The results were presented as fold change expression of the target genes, and results were presented as the mean of three independent biological isolates.

Disk Diffusion Assay

20 μl overnight culture was mixed with 5 mL melted LB top agar (0.75%) and poured on a LB agar plate. After the agar was solidified, round filter paper disks were placed. 5 μl antibiotic solution (2 mg/ml) was added to the center of the paper disks. The plates were incubated at 37°C for 16 h.

Fractional Inhibitory Concentration Index

Synergy of resistance determinants combinations was determined by calculating fractional inhibitory concentration index (FICI) values (Gonzales et al., 2015). The MIC of double or triple reverse mutations is divided by the MIC of each of single mutation, yielding the fractional contribution of each mutation in the combination. Interaction of different resistance mutations (A, B, C) is scored using the following formula: $FICI_{(ABC)} = MIC_{(ABC)}/MIC_{(A)} + MIC_{(ABC)}/MIC_{(B)} + MIC_{(ABC)}/MIC_{(C)}$.

PI-BactD Assay

Overnight *P. aeruginosa* culture was diluted to OD_{600} = 0.01 in fresh LB medium in the presence or absence of PAβN (7.5 μg/ml). Diluted cell culture was incubated at 37°C with 220-rpm agitation. Cells were harvested when OD_{600} reaches 2.0 by centrifugation and washed twice using PBS buffer (10 mM, pH 7.2). The bacterial cell pellets were re-suspended in PBS to OD_{600} as 0.4. PI-BactD was added into 1 mL cell suspension to a final concentration of 10 μM. Output signals of two channels: fluorescence increase ($\Delta S/S_0$) and fluorescence ratiometric changes (I_{482}/I_{375}) were recorded to plot the 2D graph. Six replicates were conducted for each strain and treatment.

Time-Kill Assay

The time-kill assay was performed as described by Mohamed et al. (2014). Briefly, overnight culture of PAO1 or PA154197 was diluted to 1 × 10^8 CFU/ml in LB medium and incubated with PAβN (7.5 μg/ml) and antibiotic (IPM or FOF) at certain concentration (4 MIC) at 37°C with 220-rpm agitation. 20 μL of bacterial suspensions were removed at various time intervals (1, 2, 4 h), serially diluted in PBS and plated onto LB agar plates. CFU were counted after 16-20 h incubation at 37°C. Assays were performed in triplicate.

QUANTIFICATION AND STATISTICAL ANALYSIS

Experimental replicates and other statistical information can be found in the figure legends. Quantification data presented in the figures are shown as mean ± standard deviation (SD) from three biological replicates where biological replicates (n = 3) indicate the numbers of independent, fresh bacterial colonies.

DATA AND CODE AVAILABILITY

This study did not generate/analyze [datasets/code].